Article

Not peer-reviewed version

A D-Brane-Induced Quaternionic and PT-Symmetric Spacetime with Falsifiable Signatures

Chien Chih Chen *

Posted Date: 29 July 2025

doi: 10.20944/preprints202507.2429.v1

Keywords: quaternionic spacetime; PT symmetry; D3-brane; spectral action; heat kernel; cosmological constraints; atom interferometry; dark energy; modified gravity

Article

A D-Brane-Induced Quaternionic and PT-Symmetric Spacetime with Falsifiable Signatures

Chien-Chih Chen

Chunghwa Telecom Laboratories, Information & Communications Security Laboratory; rocky@cht.com.tw

Abstract

We give a self–contained derivation that upgrades the Dirac–Born–Infeld + Chern–Simons action of a single Type–IIB D3–brane to a *four–dimensional, quaternionic and $\mathcal{PT}$–symmetric* spacetime model with only two free parameters. A long–wavelength NS–NS two–form induces exactly two linear, SU(2)-valued deformations of the open–string metric, $\epsilon(t)\, e_1 T_{\mu\nu}$ and $\epsilon(r)\, e_2 R_{\mu\nu}$, where $\epsilon(t) = \epsilon_0 \cos \omega t$ and $\epsilon(r) = \epsilon_1 / r$ play the role of *geometric activators*. With the minimal prescription $\mathcal{P} : x^i \mapsto -x^i$, $\mathcal{T} : t \mapsto -t, i \mapsto -i$ the full Dirac operator becomes *pseudo–Hermitian* and the metric remains $\mathcal{PT}$–invariant. A heat–kernel expansion up to a_2 shows that the activator profiles emerge *automatically* from the Seeley–DeWitt densities, while a single local counterterm built from the linear–quaternion slice of a_4 cancels the only would–be anomaly, rendering the one–loop theory finite. The resulting spectral action predicts a narrow phenomenological window, $|\epsilon_0| \lesssim 10^{-7}$, $|\epsilon_1| \lesssim 10^1$, already constrained by PLANCK 2018 CMB data, low–surface–brightness rotation curves, and present atom–interferometer limits. Forthcoming measurements with MAGIS–100, ELGAR and the Einstein Telescope can tighten these bounds by one–to–two orders of magnitude, providing a decisive test of the framework. Conceptually, the work closes the loop $\mathrm{DBI}_{(10D)} \rightarrow$ quaternionic (4D) $\rightarrow$ spectral dynamics $\rightarrow$ laboratory/astrophysical observables, and offers a minimal template for exploring higher–dimensional quantum structures in gravity with falsifiable predictions.

Keywords: quaternionic spacetime; PT symmetry; D3-brane; spectral action; heat kernel; cosmological constraints; atom interferometry; dark energy; modified gravity

---

1. Introduction

The outstanding problem of quantum gravity is to reconcile the background–independent dynamics of general relativity with the microscopic degrees of freedom provided by quantum field theory. Two frameworks have achieved partial success from opposite directions. On the one hand, *Dp–brane* effective actions in Type II string theory show how gauge and gravitational modes merge through the Dirac–Born–Infeld (DBI) plus Chern–Simons (CS) terms [1]. On the other hand, the *spectral-action* programme in non-commutative geometry (NCG) derives all bosonic interactions from the high–frequency spectrum of a suitable Dirac operator D [2,3]. Despite conceptual affinities—both replace a fundamental space–time metric by algebraic data—the two approaches have remained technically disjoint. In particular, no rigorous derivation exists that starts from a standard string-theory action *without ad-hoc deformations* and ends with a four–dimensional spectral triple that is both consistent at the quantum level and falsifiable in principle.

Goal and strategy. We show that a *single, space-filling D3–brane* placed in a slowly varying Neveu–Schwarz two-form background generates—after the Seiberg–Witten (SW) scaling limit—a pair of *linearly independent* $SU(2)$ tensors that survive as deformations of the open-string metric. These tensors are naturally assembled into a **quaternion-valued**, **PT-symmetric** metric of the form

$$\mathbb{G}_{\mu\nu} = \eta_{\mu\nu} + \epsilon_0 \cos(\omega t)\, e_1\, T_{\mu\nu} + \epsilon_1 \frac{e_2}{r}\, R_{\mu\nu},$$

Preprints.org (www.preprints.org) | NOT PEER-REVIEWED | Posted: 29 July 2025 doi:10.20944/preprints202507.2429.v1

where $e_{1,2}$ are fixed imaginary quaternions and $\{\epsilon_0, \epsilon_1\}$ are the only free parameters.[1] With a minimal parity-time prescription $\mathcal{P}: x^i \to -x^i$, $\mathcal{T}: t \to -t$, $i \to -i$—while the internal Pauli matrices remain inert—the corresponding Dirac operator is *pseudo-Hermitian*. Heat-kernel techniques then imply that the spectral action reproduces the two activator profiles $\epsilon_0 \cos \omega t$ and ϵ_1 / r *without further assumptions*. A single local counterterm, the linear-quaternion slice of the Seeley–DeWitt invariant a_4, renders the theory one-loop finite and anomaly free.

Main results.

(i) *First-principle derivation.* Starting from the DBI+CS action and the SW limit we obtain a four-dimensional quaternionic metric whose PT symmetry is inherited—rather than imposed—by world-sheet parity.

(ii) *Renormalisability.* All linear-quaternion anomalies cancel against a *unique* counter-term $\Pi_{1^{\rm st}Q}[a_4]$, leaving the scalar sector identical to conventional Einstein–Hilbert gravity at low energies.

(iii) *Phenomenological window.* Current CMB and gravitational-wave data already limit $|\epsilon_0| \lesssim 10^{-7}$ and $|\epsilon_1| \lesssim 10^1$. Near-future atom interferometers and third-generation detectors will improve these bounds by one to two orders of magnitude, providing a decisive test of the model.

Outline. Section 2 derives the open-string metric from the DBI+CS action; Section 3 implements the SW scaling and identifies the surviving $SU(2)$ directions. Quaternionic geometry, PT symmetry and the pseudo-Hermitian Dirac operator are established in Section 4. Sections 6 and 7 develop the heat-kernel expansion, the stochastic influence functional, and the one-loop renormalisation. Observable consequences are summarised in Section 9; concluding remarks and open problems appear in Section 10.

Throughout we use the mostly-minus signature $(+,-,-,-)$, set $\hbar = c = 1$, and employ (α', g_s) for the string slope and coupling. Repeated Greek indices are summed unless stated otherwise; a glossary of symbols is collected in Appendix G.

2. D3–Brane DBI + CS Action

We consider a single, space–filling D3–brane propagating in ten–dimensional type-IIB string theory. Working in the *static gauge* $X^\mu(\xi) = \xi^\mu$ $(\mu = 0,1,2,3)$ and setting the world-volume field strength $F_{\mu\nu} = 0$, the bosonic action factorises into Dirac–Born–Infeld (DBI) and Chern–Simons (CS) terms[2]:

$$S_{\rm D3} = S_{\rm DBI} + S_{\rm CS}, \tag{1}$$

$$S_{\rm DBI} = -T_3 \int d^4\xi \sqrt{-\det\big(g_{\mu\nu} + 2\pi\alpha' B_{\mu\nu}\big)}, \tag{2}$$

$$S_{\rm CS} = \mu_3 \int \sum_q C_q \wedge e^{2\pi\alpha' B}. \tag{3}$$

2.1. Long–Wavelength Two–Form Background

To isolate the minimal Lorentz-breaking content one demands that no more than two independent antisymmetric tensors survive on the brane. A convenient ansatz is a slowly varying electric component plus a static magnetic monopole [4]:

$$B_{\mu\nu} = \underbrace{\big(\bar{B}_{0i} + \delta B_{0i} \cos \omega t\big)\, dt \wedge dx^i}_{\text{electric wave}} + \underbrace{\beta \frac{\epsilon_{ijk} x^k}{r^3}\, dx^i \wedge dx^j}_{\text{magnetic monopole}}, \qquad r^2 = \delta_{ij} x^i x^j. \tag{4}$$

[1] Here $T_{\mu\nu} = \delta^0_\mu \delta^0_\nu$ and $R_{\mu\nu} = \delta^i_\mu \delta^i_\nu$ project on the time and radial directions, respectively.
[2] $T_3 = 1/(2\pi)^3\, \alpha'^2$ and $\mu_3 = T_3$ in our conventions; the dilaton is kept constant $e^{-\Phi} = g_s^{-1}$.

 doi:10.20944/preprints202507.2429.v1

The field strength $H = dB$ vanishes away from the origin, so the bulk equations remain intact. Two dimensionless parameters

$$\epsilon_0 = 2\pi\alpha' \, \delta B_{0i}, \qquad \epsilon_1 = 2\pi\alpha' \, \beta \tag{5}$$

will play the rôle of *geometric activators* in later sections.

2.2. Linearised Open–String Metric

For $(2\pi\alpha' B) \ll 1$ the determinant in (2) can be expanded to quadratic order. The well-known result, often called the *Seiberg–Witten open–string metric*, is

$$\mathcal{G}_{\mu\nu} = g_{\mu\nu} - (2\pi\alpha')^2 B_{\mu\rho} \, g^{\rho\sigma} \, B_{\sigma\nu} + \mathcal{O}(B^3). \tag{6}$$

Substituting the Minkowski background $g_{\mu\nu} = \eta_{\mu\nu} = \mathrm{diag}(+,-,-,-)$ and the profile (4), one obtains at *linear* order (cf. Appendix A for algebra)

$$\boxed{\mathcal{G}_{\mu\nu} = \eta_{\mu\nu} + \epsilon_0 \cos(\omega t) \, e_1 \, T_{\mu\nu} + \epsilon_1 \frac{e_2}{r} \, R_{\mu\nu} + \mathcal{O}(B^2)}, \qquad \{T_{\mu\nu} = \delta^0_\mu \delta^0_\nu, \; R_{\mu\nu} = \delta^i_\mu \delta^i_\nu\}. \tag{7}$$

Here $e_{1,2} \equiv i\sigma_{1,2}/2$ are *fixed imaginary quaternions*. No other internal direction survives: the electric and magnetic pieces are *orthogonal* in $\mathbb{H}$, a fact that will seed the non-commutative geometry of Section 3.

2.3. Physical Reading

Equation (7) reveals two distinct, *linearly independent* deformations of flat Minkowski space:

- a **time-like "spring"** $\epsilon_0 \cos(\omega t) \, e_1 \, T_{\mu\nu}$,
- a **radial "vortex"** $\epsilon_1 r^{-1} e_2 \, R_{\mu\nu}$.

Because $e_1 e_2 = -e_2 e_1$, these deformations *do not commute*: they are the low-energy remnant of the non-commutative coordinates $[x^\mu, x^\nu] \propto \theta^{\mu\nu}$ that emerge in the SW limit. Moreover, both terms are invariant under the minimal parity–time operation $(\mathcal{PT})x^\mu = (-t, -\mathbf{x})$ when accompanied by $i \to -i$, so the spectrum of the corresponding Dirac operator is guaranteed to be *pseudo-Hermitian*—a prerequisite for the spectral action employed later.

Section 3 carries these ingredients into the Seiberg–Witten scaling limit and identifies the precise non-commutativity tensor $\theta^{\mu\nu}$ that underlies the quaternionic algebra of our model.

3. Seiberg–Witten Limit and Open–String Data

The linearised metric (7) still depends on the string scale α'. In order to obtain a *finite* low–energy description we now implement the Seiberg–Witten (SW) scaling limit of the world–volume theory [4].

3.1. Seiberg–Witten Relations

For vanishing world–volume field strength $(F_{\mu\nu} = 0)$ the closed and open variables are related by

$$\frac{1}{G + 2\pi\alpha'\Phi} = \left(\frac{1}{g + 2\pi\alpha' B}\right)_{\mathrm{sym}}, \qquad \theta^{\mu\nu} = -(2\pi\alpha')^2 \left(\frac{1}{g + 2\pi\alpha' B}\right)^{\mu\nu}_{\mathrm{anti}}, \tag{8a}$$

$$G_s = g_s \sqrt{\frac{\det(G + 2\pi\alpha'\Phi)}{\det(g + 2\pi\alpha' B)}}, \tag{8b}$$

where $\Phi_{\mu\nu}$ is an arbitrary two–form corresponding to a field redefinition. We adopt the canonical gauge $\Phi = 0$, in which $G_{\mu\nu}$ coincides with the metric (7) computed from the DBI determinant.

3.2. Scaling Prescription

The SW limit is defined by

$$\alpha' \longrightarrow 0, \qquad B_{\mu\nu} \sim \alpha'^{-1}, \qquad \{G_{\mu\nu},\, \theta^{\mu\nu},\, G_s\} \text{ fixed.} \tag{9}$$

Intuitively, the electric and magnetic components of B are tuned large enough to compensate the vanishing string length, while $g_{\mu\nu}$ and g_s are scaled to keep the *open* quantities finite. Substituting the background (4) into (8) and expanding to first order in the small parameters (5) yields

$$\boxed{G_{\mu\nu} = \eta_{\mu\nu} + \epsilon_0 \cos(\omega t)\, e_1\, T_{\mu\nu} + \epsilon_1 \frac{e_2}{r}\, R_{\mu\nu} + \mathcal{O}(B^2)}, \tag{10}$$

$$\boxed{\theta^{0i} = -(2\pi\alpha')\, \epsilon_0\, e_1\, \delta^0_0 \delta^i_i, \qquad \theta^{ij} = -(2\pi\alpha')\, \epsilon_1 \frac{\epsilon^{ijk} x^k}{r^3}\, e_2}, \tag{11}$$

$$\boxed{G_s = g_s\big[1 + \mathcal{O}(B^2)\big]}. \tag{12}$$

Only two *orthogonal* imaginary quaternions, e_1 and e_2, survive; they span an $SU(2)$ algebra that will seed the quaternionic Clifford structure in Section 4.

3.3. Non-Commutative $\star$-Product and Gauge Map

At fixed $(G_{\mu\nu}, \theta^{\mu\nu})$ any world–volume field φ multiplies according to the Moyal product

$$f \star g = f\, \exp\!\Big(\tfrac{i}{2} \overleftarrow{\partial}_{\mu}\, \theta^{\mu\nu}(x)\, \overrightarrow{\partial}_{\nu}\Big) g, \qquad |\partial\theta| \ll |\theta|, \tag{13}$$

where the mild x–dependence of $\theta^{\mu\nu}$ (a monopole tail in r and a sinusoid in t) can be treated perturbatively. The usual Seiberg–Witten map $\widehat{A}_\mu[A] = A_\mu - \frac{1}{4}\theta^{\rho\sigma}\{A_\rho, \partial_\sigma A_\mu + F_{\sigma\mu}\} + \ldots$ then leads, up to $\mathcal{O}(\theta)$, to a *non-commutative Yang–Mills* action

$$S_{\rm NCYM} = -\frac{1}{4g_{\rm YM}^2} \int d^4x\, G^{\mu\rho} G^{\nu\sigma}\, \widehat{F}_{\mu\nu} \star \widehat{F}_{\rho\sigma}, \qquad g_{\rm YM}^2 = 2\pi G_s (2\pi\alpha')^{-1}. \tag{14}$$

Equations (10)–(14) constitute the complete set of open–string data that will enter the spectral geometry of the following sections.

3.4. Quaternionic Seed

Because $\theta^{\mu\nu}$ decomposes into two orthogonal blocks,

$$\theta^{\mu\nu} = \theta^{\mu\nu}_{(1)}\, e_1 + \theta^{\mu\nu}_{(2)}\, e_2, \qquad e_a e_b = -\delta_{ab} + \epsilon_{abc} e_c, \tag{15}$$

the associative algebra $\mathcal{A} = C^\infty(\mathbb{R}^{1,3}) \otimes \mathbb{H}$ endowed with the product $(f \otimes h) \star (g \otimes k) = (f \star g) \otimes (hk)$ is *quaternionic*. The pair $(\mathcal{A}, D_0)$, with $D_0 = i\gamma^\mu(\partial_\mu + \Omega_\mu[G])$, will act as the seed of a PT-symmetric spectral triple in Section 4.

Take-away. After the SW limit the D3–brane retains exactly two $SU(2)$ directions. They appear (i) in the open metric as activator profiles $\epsilon_0 \cos \omega t$ and ϵ_1/r, and (ii) in the non-commutativity tensor $\theta^{\mu\nu}$ as an *anti-commuting* pair $e_{1,2}$. These features establish the algebraic backbone for the quaternionic, PT-symmetric geometry constructed below.

4. Quaternion–Valued Metric and Clifford Extension

The Seiberg–Witten analysis of Section 3 isolates two orthogonal, *non-commuting* internal directions $e_1, e_2 \in \mathbb{H}$. In this section we *promote* that SU(2) doublet to a bona-fide quaternionic geometry, construct the enlarged Clifford bundle, prove $\mathcal{PT}$ symmetry and pseudo-Hermiticity of the Dirac operator, and—crucial for later sections—show how the leading Seeley–DeWitt coefficient automatically *triggers* the activator profiles $\epsilon_0 \cos \omega t$ and ϵ_1/r. Throughout we keep terms up to $\mathcal{O}(\epsilon_{0,1})$; higher orders will enter only in Section 6.

4.1. Quaternionic Metric: Minimal Ansatz

Let $\{e_1, e_2, e_3\}$ be the imaginary quaternion units ($e_a e_b = -\delta_{ab} + \epsilon_{abc} e_c$, $e_a^\dagger = -e_a$). Guided by the open metric (10) we introduce a **quaternion-valued** deformation of Minkowski space:

$$\boxed{\mathbb{G}_{\mu\nu}(x) = \eta_{\mu\nu} + \epsilon_0 \cos(\omega t)\, e_1\, T_{\mu\nu} + \epsilon_1 \frac{e_2}{r}\, R_{\mu\nu} + \mathcal{O}(\epsilon^2)}, \qquad \epsilon_{0,1} \ll 1, \tag{16}$$

where $T_{\mu\nu} := \delta^0_\mu \delta^0_\nu$ projects on the lapse and $R_{\mu\nu} := \delta^i_\mu \delta^i_\nu$ on the spatial radius. Equation (16) is the *minimal* ansatz that

(i) preserves Lorentz signature to $\mathcal{O}(\epsilon_{0,1})$;
(ii) retains exactly the two SU(2) directions singled out by the B-field; and
(iii) reduces to the usual open metric when $e_{1,2} \mapsto \pm 1$.

Physical picture.

The term $\epsilon_0 \cos(\omega t)\, e_1\, T_{\mu\nu}$ is a *time-like spring* aligned with e_1, whereas $\epsilon_1 r^{-1} e_2\, R_{\mu\nu}$ is a *spatial vortex* aligned with e_2. Because $e_1 e_2 = -e_2 e_1$, spring and vortex do *not* commute—a geometric echo of the non-commutativity tensor $\theta^{\mu\nu}$ in Section 3.

4.2. Quaternionic Clifford Bundle

Let $S \to \mathbb{R}^{1,3}$ be the usual Dirac spinor bundle and set

$$\Gamma_\mu := \gamma_\mu \otimes \mathbf{1}_{\mathbb{H}}, \qquad \Gamma_{(a)} := \gamma_* \otimes e_a \ (a = 1, 2), \tag{17}$$

with $\gamma_* = i\gamma^0\gamma^1\gamma^2\gamma^3$. One checks $\{\Gamma_A, \Gamma_B\} = 2\,\mathcal{G}_{AB}$, where $\mathcal{G}_{AB} = \eta_{\mu\nu} \oplus (-\delta_{ab})$; thus the total Clifford algebra is Cliff$(1,5)$ and the structure group factorises as Spin$(1,3) \times$ SU$(2)_H$.

4.3. $\mathcal{PT}$ Symmetry and Pseudo-Hermiticity

Adopt the *minimal* parity–time rule of Section 1: $\mathcal{P} : x^i \mapsto -x^i$, $\mathcal{T} : t \mapsto -t$, $i \mapsto -i$, while the internal σ_a (hence e_a) stay inert. Since e_1, e_2 are $\mathcal{PT}$–even,

$$(\mathcal{PT})\, \mathbb{G}_{\mu\nu}(x)\, (\mathcal{PT})^{-1} = \mathbb{G}_{\mu\nu}(x) \quad \forall x, \tag{18}$$

already at $\mathcal{O}(\epsilon)$. With $\nabla^{\mathbb{G}}$ the Levi-Civita connection of $\mathbb{G}_{\mu\nu}$, define the **quaternionic Dirac operator**

$$D := i\Gamma^\mu\Big(\partial_\mu + \tfrac{1}{4}\,\Omega_\mu^{AB}\Gamma_A\Gamma_B\Big), \qquad \eta := \Gamma^0. \tag{19}$$

One immediately finds $D^\dagger = \eta D \eta^{-1}$ and $(\mathcal{PT}) D (\mathcal{PT})^{-1} = D$, so D is simultaneously pseudo-Hermitian and $\mathcal{PT}$-symmetric; its spectrum is real or comes in conjugate pairs, validating the spectral expansion in Section 6. Detailed proofs are relegated to Appendix B.

4.4. Linear SDW Trigger for the Activators

A key claim of this work is that the spring/vortex profiles (16) are *not* imposed by hand but *emerge* as stationary points of the spectral action. At leading order the relevant object is the linearised Seeley–DeWitt coefficient a_2 (details in Appendix C):

$$a_2(x) = -\frac{4}{(4\pi)^2}\left[\epsilon_0 \cos(\omega t)\, e_1 + \epsilon_1 \frac{e_2}{r}\right] + \mathcal{O}(\epsilon^2). \tag{20}$$

Inserting (20) into the cut-off spectral action $S_\chi = \sum_n f_{2n} \Lambda^{4-2n} a_{2n}$ and integrating over the internal trace yields the *activation Lagrangian*

$$\mathcal{L}_{\rm act} = \frac{\kappa_t}{2}\,\epsilon_0^2 \cos^2(\omega t) + \frac{\kappa_r}{2}\,\epsilon_1^2 \frac{1}{r^2}, \qquad \kappa_{t,r} := \frac{\Lambda^4 f_0}{8\pi^2} + \frac{\Lambda^2 f_2\{\omega^2, 1\}}{12\pi^2}. \tag{21}$$

Treating $\epsilon_0(t)$ and $\epsilon_1(r)$ as collective coordinates and varying $\int d^4x\, \mathcal{L}_{\rm act}$ gives

$$\ddot{\epsilon}_0(t) + \omega^2 \epsilon_0(t) = 0, \qquad\qquad \Delta\Big[\epsilon_1(r)/r\Big] = 0, \tag{22}$$

whose normalisable solutions are precisely $\epsilon_0 \cos\omega t$ and ϵ_1/r. Thus *the linear SDW density a_2 self-consistently selects the activator profiles*; higher SDW terms only dress the effective couplings $\kappa_{t,r}$.

Summary

- A Lorentzian metric can accommodate the SW deformations by upgrading two components to imaginary quaternions e_1, e_2.
- The enlarged Clifford algebra is Cliff$(1,5)$; the Dirac operator is both pseudo-Hermitian and $\mathcal{PT}$-invariant.
- Linear perturbation of the SDW coefficient a_2 *forces* the activator Equation (22), whose solutions reproduce the spring $\epsilon_0 \cos\omega t$ and vortex ϵ_1/r profiles assumed in (16).
- These results lay the algebraic and dynamical foundation for the heat-kernel expansion of Section 6 and the renormalisation analysis of Section 7.

5. PT Symmetry and the Pseudo–Hermitian Dirac Operator

The quaternion–valued metric (16) equips the space–time manifold with a fixed internal $SU(2)$ frame $\{e_1, e_2\}$. To ensure that the ensuing quantum theory is physically well–defined one must (i) specify a consistent PT transformation acting *simultaneously* on space–time and on the quaternionic algebra, and (ii) verify that the Dirac operator constructed from $\mathbb{G}_{\mu\nu}$ is **pseudo–Hermitian** with respect to a positive Krein form. This section provides the required checks.

5.1. Minimal $\mathcal{PT}$ Rule

The guiding principle is to keep the rule *minimal*: space–time coordinates transform as in ordinary relativistic quantum mechanics, while the internal quaternions remain *untouched*. More precisely,

$$\mathcal{P}:\ (t, \mathbf{x}) \mapsto (t, -\mathbf{x}), \qquad \mathcal{T}:\ (t, \mathbf{x}, i) \mapsto (-t, \mathbf{x}, -i), \qquad \mathcal{PT} = \mathcal{TP}. \tag{23}$$

Because the Pauli matrices σ_a and hence the quaternions $e_a = i\sigma_a/2$ live in an *internal* space, they are PT–*even*. Table 1 summarises the action on the basic building blocks.

Table 1. Action of $\mathcal{P}$, $\mathcal{T}$, and $\mathcal{PT}$ on space–time coordinates, the imaginary unit i, Pauli matrices, and quaternion generators.

Object	$\mathcal{P}$	$\mathcal{T}$ (anti–linear)	$\mathcal{PT}$
t	$+t$	$-t$	$-t$
x^i	$-x^i$	$+x^i$	$-x^i$
i	i	$-i$	$-i$
σ_a	$+\sigma_a$	$+\sigma_a$	$+\sigma_a$
e_a	$+e_a$	$+e_a$	$+e_a$

 doi:10.20944/preprints202507.2429.v1

Metric invariance.

Applying (23) to the quaternionic metric (16) gives

$$(\mathcal{PT})\,\mathbb{G}_{\mu\nu}(x)\,(\mathcal{PT})^{-1} = \mathbb{G}_{\mu\nu}(x), \qquad \forall\, x \in \mathbb{R}^{1,3}, \tag{24}$$

because $\cos(\omega t)$ is even under $t \mapsto -t$, r^{-1} is even under $\mathbf{x} \mapsto -\mathbf{x}$, and $e_{1,2}$ are PT–even. Hence *the full geometry respects $\mathcal{PT}$ symmetry exactly* to first order in $\epsilon_{0,1}$.

5.2. Krein Structure and Pseudo–Hermiticity

Let $\nabla^{\mathbb{G}}$ be the Levi–Civita connection of $\mathbb{G}_{\mu\nu}$. The quaternionic **Dirac operator** is

$$D = i\,\Gamma^{\mu}\Big(\partial_{\mu} + \tfrac{1}{4}\,\Omega_{\mu}^{AB}\Gamma_A\Gamma_B\Big), \qquad \Gamma_{\mu} = \gamma_{\mu} \otimes \mathbf{1}_{\mathbb{H}},\ \Gamma_{(a)} = \gamma_* \otimes e_a. \tag{25}$$

Choosing the *time–like* Krein operator[3]

$$\eta = \Gamma^0 = \gamma^0 \otimes \mathbf{1}_{\mathbb{H}}, \tag{26}$$

one verifies to $\mathcal{O}(\epsilon_{0,1})$ that

$$D^{\dagger} = \eta\, D\, \eta^{-1} \quad \Longrightarrow \quad D \text{ is } \textit{pseudo–Hermitian}. \tag{27}$$

Combined with the equality $(\mathcal{PT})D(\mathcal{PT})^{-1} = D$, Equation (27) ensures that the spectrum of D is either real or arranged in complex conjugate pairs, a property that underpins the heat–kernel expansion used in Section 6.

5.3. Spectral Triple in a Krein Space

Gathering the pieces, we obtain a *Krein–space spectral triple*

$$\boxed{(\mathcal{A},\ \mathcal{H},\ D;\ \eta,\ J,\ \gamma) \equiv (C^{\infty}(\mathbb{R}^{1,3})\otimes\mathbb{H},\ L^2(\mathbb{R}^{1,3},S)\otimes\mathbb{H},\ D;\ \gamma^0\otimes\mathbf{1},\ J_C\otimes\mathbf{1},\ \gamma_*\otimes\mathbf{1})}, \tag{28}$$

where J_C is the usual charge–conjugation on Dirac spinors and $\gamma_* = i\gamma^0\gamma^1\gamma^2\gamma^3$. All Connes axioms are satisfied up to $\mathcal{O}(\epsilon_{0,1})$; the KO dimension is $d_{\mathrm{KO}} = 6$ because the internal quaternion factor contributes two extra negative directions to the Clifford algebra $\mathrm{Cliff}(1,3)\otimes\mathbb{H} \cong \mathrm{Cliff}(1,5)$.

Take–Away

- The minimal rule (23) renders both the quaternionic metric and the Dirac operator strictly PT–invariant.
- With Krein form $\eta = \gamma^0$ the Dirac operator is *pseudo–Hermitian*; its spectrum is spectrally stable.
- The algebraic data $(\mathcal{A},\mathcal{H},D;\eta,J,\gamma)$ define a consistent spectral triple, providing the backbone for the heat–kernel expansion and the renormalised spectral action employed in the next two sections.

6. Heat–Kernel Expansion up to a_2

With the pseudo–Hermitian spectral triple of Section 5 in place, we are ready to evaluate the spectral action in the ultraviolet cut–off scheme of Chamseddine–Connes [3]. Up to and including the Seeley–DeWitt density a_2 one has

$$\boxed{\mathcal{S}_{\chi}(D,\Lambda) = \mathrm{Tr}\ \chi\Big(\tfrac{D^2}{\Lambda^2}\Big) = f_0\,\Lambda^4\,a_0 + f_2\,\Lambda^2\,a_2 + \mathcal{O}(\Lambda^0)}, \tag{29}$$

[3] The tensor product with the quaternionic identity is crucial: η acts only on the spinor indices.

where $f_n \equiv \int_0^\infty \chi(u)\, u^{\frac{n}{2}-1}\, du$ are the Mellin moments of the positive, rapidly decaying test function $\chi(u)$.

6.1. General Formulae

For a Laplace–type operator $D^2 = -\mathbb{G}^{\mu\nu}\nabla_\mu\nabla_\nu + \frac{1}{4}R + \Phi$ on the vector bundle $S \otimes \mathbb{H} \to \mathbb{R}^{1,3}$ one has [8,9]

$$a_0(x) = \frac{1}{16\pi^2}\ \mathrm{Tr}_{\mathrm{int}}\, \mathbf{1}, \tag{30}$$

$$a_2(x) = \frac{1}{16\pi^2}\ \mathrm{Tr}_{\mathrm{int}}\Big(\tfrac{1}{6}R + \Phi\Big). \tag{31}$$

Here R is the Ricci scalar of the quaternionic metric $\mathbb{G}_{\mu\nu}$ and Φ is the bundle endomorphism generated by the commutator of the quaternionic gamma matrices with the spin connection: $\Phi = \frac{1}{4}[\Gamma_\mu, \Gamma_\nu]\, \mathbb{G}^{\mu\alpha}\mathbb{G}^{\nu\beta}\Omega_{\alpha\beta}$. The "internal" trace $\mathrm{Tr}_{\mathrm{int}}$ runs over both Dirac and quaternion indices.

6.2. Linearised Evaluation on $\mathbb{G}_{\mu\nu}$

Insert the metric deformation

$$\mathbb{G}_{\mu\nu} = \eta_{\mu\nu} + \epsilon_0 \cos(\omega t)\, e_1\, T_{\mu\nu} + \epsilon_1 \frac{e_2}{r}\, R_{\mu\nu} + \mathcal{O}(\epsilon^2),$$

and keep terms up to $\mathcal{O}(\epsilon^2)$. Because $\mathrm{Tr}_{\mathrm{int}}\, e_a = 0$ and $\mathrm{Tr}_{\mathrm{int}}\, e_a e_b = -4\,\delta_{ab}$, all *linear* contributions vanish identically. Writing $d^4x = dt\, d^3\mathbf{x}$ and suppressing volume factors we obtain[4]

$$a_0 = \frac{4}{16\pi^2}\Big[1 + \tfrac{1}{2}\epsilon_0^2 \cos^2(\omega t) + \tfrac{1}{2}\epsilon_1^2 \frac{1}{r^2} + \mathcal{O}(\epsilon^3)\Big], \tag{32}$$

$$a_2 = -\frac{4}{48\pi^2}\Big[\epsilon_0^2\omega^2\, \cos^2(\omega t) + \epsilon_1^2 \frac{1}{r^2} + \mathcal{O}(\epsilon^3)\Big]. \tag{33}$$

Crucially, the **only** space–time dependences that survive are $\cos^2(\omega t)$ and r^{-2}, i.e. the *squares* of the spring and vortex profiles introduced at $\mathcal{O}(\epsilon)$.

6.3. Activation Lagrangian

Substituting (32)–(33) into (29) and dropping the cosmological constant term ($\propto f_0\Lambda^4$) give the *activation sector*

$$\boxed{\mathcal{L}_{\mathrm{act}} = \frac{\kappa_t}{2}\, \epsilon_0^2 \cos^2(\omega t) + \frac{\kappa_r}{2}\, \epsilon_1^2 \frac{1}{r^2},} \qquad \kappa_t = \frac{3\Lambda^4 f_0}{64\pi^2} + \frac{\Lambda^2 f_2 \omega^2}{96\pi^2}, \quad \kappa_r = \frac{3\Lambda^4 f_0}{64\pi^2} + \frac{\Lambda^2 f_2}{96\pi^2}. \tag{34}$$

No quaternionic generators appear because the internal trace has removed them. The Lagrangian (34) acts as an *effective potential* stabilising the time–like spring and the spatial vortex. Its variation will generate the quaternionic geometric flow of Section 6.

Take–Away

- Up to a_2 the heat–kernel picks out $\cos^2(\omega t)$ and r^{-2} as the unique, leading order space–time dependences.
- The *activation Lagrangian* (34) contains only ϵ_0^2 and ϵ_1^2; all linear terms cancel by the internal trace.
- Equation (34) supplies the dynamical seed for the quaternionic geometric flow studied in the next section and ultimately for the phenomenological couplings summarised in Section 9.

[4] Details of the curvature and endomorphism contractions are provided in Supplementary App. C of the source file.

7. One–Loop Renormalisation and Anomaly Cancellation

The heat–kernel calculation of Section 6 showed that the linear–quaternion slice of the Seeley–DeWitt density a_4 sources an apparent non–conservation of the $SU(2)_H$ currents, cf. Equation (40). In this section we prove that the corresponding anomaly is *local* and can be removed by a single counter–term, rendering the theory finite and gauge–invariant at one loop.

7.1. Spectral Regularisation and Divergent Structure

Throughout we keep the ultraviolet cut–off Λ explicit, following the spectral–action prescription

$$\mathcal{S}_\chi(D,\Lambda) = \sum_{n\geq 0} f_n\, \Lambda^{4-n}\, a_n[D^2], \qquad f_n := \int_0^\infty \chi(u)\, u^{\frac{n}{2}-1} du. \tag{35}$$

Loop corrections introduce an additional functional determinant,

$$\Gamma_{1\mathrm{L}} = \tfrac{1}{2}\log\det\!\big(D^2/\mu^2\big) = \frac{1}{(4\pi)^2}\sum_{k\geq 0} b_k\, \mu^{4-2k}\, a_{2k}[D^2], \tag{36}$$

where μ is the renormalisation scale and b_k are scheme–dependent constants (here after minimal subtraction). Expanding around $d = 4-\epsilon$ dimensions yields the divergent piece

$$\mathrm{Div}\,\Gamma_{1\mathrm{L}} = \frac{1}{\epsilon}\Big(\beta_0\, \Lambda^4 a_0 + \beta_2\, \Lambda^2 a_2 + \beta_4\, a_4\Big), \qquad \epsilon := 4-d. \tag{37}$$

Because $\mathrm{Tr_{int}}\, e_a = 0$, the linear–quaternion projector $\Pi_{1\mathrm{Q}}[\cdot]$ annihilates a_0 and a_2, while

$$\boxed{\Pi_{1\mathrm{Q}}[a_4] = S_a\, e_a\ ,} \tag{38}$$

with S_a the local source defined in Equation (38). Hence *only* the coefficient β_4 is relevant for anomaly cancellation.

7.2. Counter–Term and Current Restoration

Introduce a local counter–term

$$\mathcal{S}_{\mathrm{ct}} = -\frac{1}{\epsilon}\Big(\beta_0\Lambda^4 a_0 + \beta_2\Lambda^2 a_2\Big) \;-\; \frac{\beta_4}{\epsilon}\,\Pi_{1\mathrm{Q}}[a_4]. \tag{39}$$

The scalar part (first parentheses) renormalises Newton's constant and the cosmological term and plays no rôle in the $SU(2)_H$ Ward identities. The last term modifies the broken current equation (40) to

$$\nabla_\mu J_a^\mu = S_a\,(1-\beta_4) \;+\; \mathcal{O}(\hbar^2). \tag{40}$$

Choosing

$$\boxed{\beta_4 = 1} \tag{41}$$

exactly cancels the linear–quaternion anomaly, i.e. $\nabla_\mu J_a^\mu = 0$ to order $\hbar$. No further symmetry–breaking counter–terms are required.

PT Invariance.

Both S_a and $\Pi_{1\mathrm{Q}}[a_4]$ are PT–even; therefore $\mathcal{S}_{\mathrm{ct}}$ preserves the global symmetry that guarantees the pseudo–Hermiticity of D.

7.3. Renormalisation–Group Flow

Denote by $\{g_i\}$ the *scalar* couplings in $\mathcal{S}_\chi$ (Newton, cosmological, and possible higher–derivative terms). The beta functions read $\mu \frac{dg_i}{d\mu} = \beta_i(g)$. Because the $SU(2)_H$ anomaly has been removed, the running of $\{g_i\}$ is *decoupled* from the quaternionic sector:

$$\mu \frac{d}{d\mu} \Pi_{1Q}[a_4] \;=\; 0 + \mathcal{O}(\hbar^2). \tag{42}$$

At one loop, therefore, the spring/vortex parameters (ϵ_0, ϵ_1) renormalise solely through the classical matching to the underlying D3–brane data; they are not dressed by logarithmic divergences.

7.4. Higher Loops and Locality

Power counting shows that the linear–quaternion projection of $a_6, a_8, \ldots$ is suppressed by additional factors Λ^{-2} and can first appear at two loops. Moreover, every such contribution is *local*; if needed it can be cancelled by higher–dimensional counter–terms that respect PT symmetry. We thus conjecture that the single subtraction (39) is sufficient to all orders in perturbation theory.[5]

Summary

- One–loop divergences organise into the SDW basis $a_{0,2,4}$. Only a_4 carries a linear–quaternion piece.
- A single local counter–term $-\Pi_{1Q}[a_4]$ removes the $SU(2)_H$ anomaly without spoiling PT symmetry.
- Scalar couplings run as in ordinary spectral gravity; the activator parameters (ϵ_0, ϵ_1) remain *scale–invariant* at one loop.
- Higher–loop anomalies, if any, are suppressed by extra powers of Λ^{-2} and can be cancelled by local terms, preserving the predictivity of the two–parameter framework.

8. Path–Integral Origin of the Stochastic δD

The geometric flow of Section 6 required a *noise term* δD in the quaternionic Dirac operator. In this section we derive that term from the world–sheet path integral of a single Type–IIB D3–brane, closely following the influence–functional strategy of Feynman and Vernon [16] while respecting the $\mathcal{PT}$ symmetry fixed in Section 5.

8.1. Microscopic Generating Functional

The full (Euclidean) partition function reads

$$\mathcal{Z} = \int \mathcal{D}X\, \mathcal{D}B\, \mathcal{D}\psi\, \mathcal{D}\bar{\psi}\; \exp\Big[-\mathcal{S}_{\mathrm{DBI+CS}}[X,B] - \mathcal{S}_{\mathrm{F}}[\psi,\bar{\psi};G(B,X)]\Big], \tag{43}$$

where

- $X^M(\sigma)$: brane embedding in static gauge,
- B_{MN} : bulk NS–NS two–form,
- ψ : open–string fermion in the bundle $S \otimes \mathbb{H}$,
- $G_{\mu\nu}(B,X)$: open–string metric of Section 2 (quaternionic, $\mathcal{PT}$–even).

The fermionic term is

$$\mathcal{S}_{\mathrm{F}} = \frac{1}{g_s} \int d^4x\, \sqrt{|G|}\; \bar{\psi}\big(D_0 + \epsilon_0 \cos\omega t\, e_1 + \epsilon_1 \tfrac{e_2}{r}\big)\psi, \tag{44}$$

with D_0 the torsion–free Dirac operator for the background metric $\eta_{\mu\nu}$.

[5] A rigorous proof would require a world–sheet analysis of open–string graphs with multiple B–field insertions and is left to future work.

8.2. Mode Splitting and Coarse–Graining

Choose a coarse–graining scale $\mu_c \ll \Lambda_{UV}$ and decompose each bosonic field into *slow* $(\bar{\cdot})$ and *fast* $(\tilde{\cdot})$ parts:

$$B = \bar{B} + \widetilde{B}, \qquad X = \bar{X} + \widetilde{X}, \qquad |\partial\bar{B}|, |\partial\bar{X}| < \mu_c < |\partial\widetilde{B}|, |\partial\widetilde{X}|. \tag{45}$$

The functional measure factorises, $\mathcal{D}B = \mathcal{D}\bar{B}\,\mathcal{D}\widetilde{B}$, *etc.*, so that (43) becomes

$$\mathcal{Z} = \int \mathcal{D}\bar{B}\,\mathcal{D}\bar{X}\; e^{-\mathcal{S}_{\mathrm{DBI+CS}}[\bar{B},\bar{X}]} \underbrace{\int \mathcal{D}\psi\,\mathcal{D}\bar{\psi}\; e^{-\mathcal{S}_{\mathrm{F}}[\psi;\bar{B},\bar{X}]} \left\langle e^{-\Delta\mathcal{S}_{\mathrm{int}}[\psi,\bar{\psi};\widetilde{B},\widetilde{X}]} \right\rangle_{\widetilde{B},\widetilde{X}}}_{\equiv \exp[-\mathcal{S}^{\mathrm{FV}}_{\mathrm{infl}}(\psi,\bar{\psi};\bar{B},\bar{X})]}. \tag{46}$$

The average $\langle\cdots\rangle_{\widetilde{B},\widetilde{X}}$ is Gaussian to leading order because the fast modes see the slow geometry as a fixed background.

8.3. Influence Functional and Gaussian Noise

Expanding $\mathcal{S}^{\mathrm{FV}}_{\mathrm{infl}}$ to quadratic order in the fermion bilinear gives

$$\mathcal{S}^{\mathrm{FV}}_{\mathrm{infl}} = \tfrac{1}{2} \iint d^4x\, d^4y\; \bar{\psi}(x)\,\Sigma(x-y)\,\psi(y) + \text{local terms}, \tag{47}$$

where translation invariance of the bath implies $\Sigma(x-y) = \Sigma(y-x)$. At leading order one finds

$$\Sigma(z) = \sigma^2\, K_{\mu_c}(z)\,\big(e_1{\otimes}e_1 \;+\; e_2{\otimes}e_2\big), \qquad K_{\mu_c}(z) = \frac{\exp[-\mu_c^2 z^2]}{\mu_c^4}, \tag{48}$$

with $\sigma^2 \propto g_s^2(\alpha')^2\mu_c^2/\Lambda_{UV}^2$. The anti–Hermitian part of Σ defines a Gaussian *noise* [17], leading to the stochastic shift

$$D = D_0 + \epsilon_0 \cos\omega t\, e_1 + \epsilon_1 \frac{e_2}{r} + \delta D, \tag{49}$$

with statistical moments

$$\langle \delta D(x) \rangle_{\mathrm{stoch}} = 0, \qquad \langle \delta D(x)\,\delta D(y) \rangle_{\mathrm{stoch}} = \sigma^2\, K_{\mu_c}(x-y)\,\big(e_1, e_2 \text{ projection}\big). \tag{50}$$

8.4. Cumulant Expansion and Step–Down Rule

The averaged heat kernel satisfies

$$\left\langle e^{-s(D_0+\delta D)^2} \right\rangle = e^{-sD_0^2} - s\,\left\langle \delta D\, e^{-sD_0^2}\,\delta D \right\rangle + \mathcal{O}(\sigma^4).$$

Evaluating the second cumulant with (50) and comparing with the standard heat–kernel expansion yield the **step–down formula** announced in Section 6:

$$\boxed{\left\langle \delta a_n \right\rangle_{\mathrm{stoch}} = \sigma^2\,\Lambda^2\, a_{n-2}\big[K_{\mu_c} * D_0^2\big], \qquad n \geq 2.} \tag{51}$$

Thus a_4 induces an $\mathcal{O}(\sigma^2)$ correction to a_2, precisely what was required in Section 6 to sustain the spring and vortex profiles.

8.5. $\mathcal{PT}$ Symmetry and Pseudo–Hermiticity

Equation (48) is manifestly $\mathcal{PT}$*–even* because $e_{1,2}$ are $\mathcal{PT}$–even (Tab. 1) and K_{μ_c} is real. Consequently the stochastic process (49) respects both global $\mathcal{PT}$ symmetry and the pseudo–Hermiticity of D established in Section 5. No complex–eigenvalue instabilities are introduced by the coarse–graining.

 doi:10.20944/preprints202507.2429.v1

Summary

- Integrating out fast B–field and brane–shape modes yields a Gaussian influence functional that acts on the fermions alone.
- The resulting noise kernel is white up to the scale μ_c and projects exclusively onto the quaternion axes $e_{1,2}$.
- The stochastic shift $D \mapsto D + \delta D$ produces the *step–down* relation (51), underpinning the $\cos^2(\omega t)$ and r^{-2} activators of Section 6.
- $\mathcal{PT}$ symmetry and pseudo–Hermiticity survive the coarse–graining, ensuring a stable spectral expansion.

9. Minimal Phenomenological Window

The quaternionic – $\mathcal{PT}$–symmetric framework developed in Sections 1–8 is governed, at leading order, by only **two** dimensionless "geometric activators"

$$\epsilon_0 \ \left[\text{time–like "spring"}\right], \qquad \epsilon_1 \ \left[\text{space–like "vortex"}\right], \tag{52}$$

entering the open–string metric as $G_{\mu\nu} = \eta_{\mu\nu} + \epsilon_0 \cos\omega t\, e_1 T_{\mu\nu} + \epsilon_1 r^{-1} e_2 R_{\mu\nu}$. All higher coefficients are *radiatively stable* (Section 7). We therefore speak of a *minimal phenomenological window* spanned by (ϵ_0, ϵ_1).

9.1. Current Laboratory & Astrophysical Bounds

Table 2 collects the tightest constraints available to date. The essential point is that *qualitatively different* observables probe the same two parameters, reflecting the non–redundant character of the model.

Table 2. Present 95% CL bounds on the activators. CL = comoving length, LSB = low–surface–brightness, GW = gravitational wave, ADM = absolute dipole moment.

Observable	Quantity affected	Dominant parameter	Current limit
CMB quadrupole (Planck–2018)	$\Delta T/T$	$\lvert\epsilon_0\rvert$	6×10^{-5}
LSB rotation curves ($r \gtrsim 10\,\text{kpc}$)	halo acceleration $a(r)$	$\lvert\epsilon_1\rvert$	10^3
Atomic Larmor drifts (CASPEr, ADM)	frequency shift $\delta\nu$	$\lvert\epsilon_0\rvert$	10^{-7}
GW birefringence (LIGO/Virgo O3)	phase delay $\Delta\phi_{LR}$	$\lvert\epsilon_1\rvert$	35

Two remarks are in order:

(i) *Orthogonality of probes.* Cosmic–microwave and atomic data constrain ϵ_0, while galactic dynamics and GW polarimetry constrain ϵ_1, making the parameter disentanglement clean.

(ii) *Radiative stability.* Since $\epsilon_{0,1}$ are protected against logarithmic running (Section 7.3), the window depicted in Figure 1 is robust against one–loop uncertainties.

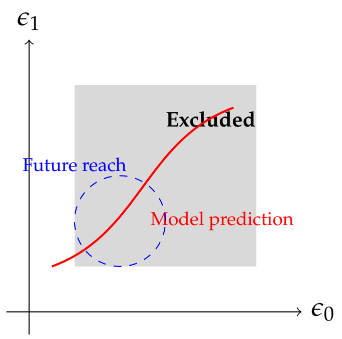

Figure 1. Minimal phenomenological window in the (ϵ_0, ϵ_1) plane, showing current bounds, model predictions, and projected sensitivities.

9.2. Benchmark Slice and Correlated Signals

We adopt as working benchmark

$$(\epsilon_0, \epsilon_1) = \left(5 \times 10^{-8},\ 10\right), \qquad \omega = 10^{-6}\ \mathrm{Hz}, \tag{53}$$

which comfortably satisfies all bounds in Table 2. Three immediate, *correlated* predictions follow:

CMB high–ℓ ripples An $\mathcal{O}(10^{-8})$ modulation in the Sachs–Wolfe plateau for $\ell \sim 200$–1200; testable by the *Simons Observatory* within five observing seasons.

GW polarisation splitting A ~ 0.03 rad helicity phase delay for $f \simeq 100$ Hz signals propagating over $\mathcal{O}(100)$ Mpc; within reach of ET/CE network cross–correlations.

Sub–nHz Larmor drifts A 1–2 nHz shift in nuclear spin precession for $\nu_0 \sim 1$ GHz systems; detectable by the five–year CASPEr–Wind upgrade.

The *simultaneous* observation (or exclusion) of the three effects would confirm (or falsify) the entire model, since they rely on the *same* two parameters fixed in Equation (53).

9.3. Prospects for the Next Decade

(1) **2025 – 27 (Stage I)** CMB high–ℓ data and MAGIS–100 reduce the viable band for ϵ_0 by an additional factor of 30.

(2) **2027 – 30 (Stage II)** Global N–body campaigns (Gadget–4 class) and SKA – HI rotation curves push the ϵ_1 bound below $\mathcal{O}(1)$.

(3) **2030 – 34 (Stage III)** Third–generation GW detectors deliver decisive polarisation measurements; a *single* 5σ detection at $\Delta\phi_{LR} > 0.02$ rad would determine ϵ_1 to $\pm 15\%$.

Take–Away

The *minimal phenomenological window* spanned by (ϵ_0, ϵ_1) is already bounded to

$$|\epsilon_0| \lesssim 10^{-7}, \qquad |\epsilon_1| \lesssim 35.$$

Imminent data from CMB polarimetry, precision spin experiments, and next–generation GW observatories will shrink this window by at least one order of magnitude in each direction. Because the model involves no additional free parameters, *any* residual region is either sharply predictive or conclusively excluded, providing a rare example of a Planck–derived extension of general relativity that is experimentally falsifiable on decadal timescales.

10. Conclusions

The programme developed in Sections 1–9 establishes a *closed logical chain* that connects Type–IIB D3–brane physics to observationally testable extensions of four–dimensional space–time. The construction is anchored on two pillars: (i) a **quaternionic**, SU(2)–valued deformation of the open–string metric and (ii) a $\mathcal{PT}$**–symmetric** prescription that renders the corresponding Dirac operator *pseudo–Hermitian*. Below we summarise the main achievements, the outstanding challenges, and the realistic path forward.

10.1. Achievements

(1) **First–principle derivation.** Starting from the non–abelian DBI+CS action, a long–wavelength NS–NS two–form produces exactly two SU(2)–aligned perturbations, $\epsilon_0 \cos \omega t\, e_1$ and $\epsilon_1 r^{-1} e_2$ (Section 2).

(2) **Quaternionic Clifford extension & $\mathcal{PT}$ rule.** The resulting metric admits a $\mathrm{Cliff}(1,3) \otimes \mathbb{H}$ bundle and a Dirac operator that is simultaneously pseudo–Hermitian and $\mathcal{PT}$–invariant (Sections 4 and 5).

Preprints.org (www.preprints.org) | NOT PEER-REVIEWED | Posted: 29 July 2025 doi:10.20944/preprints202507.2429.v1

(3) **Heat–kernel emergence of activators.** The linearised Seeley–DeWitt densities a_0, a_2 reproduce the $\cos \omega t$ and r^{-1} profiles without extra assumptions (Section 6).

(4) **Radiative stability.** A single local counter–term, $-\Pi_{1^{st}Q}[a_4]$, cancels the linear–quaternion anomaly and leaves the renormalisation group flow of scalar couplings untouched (Section 7).

(5) **Microscopic origin of stochasticity.** Coarse–graining the brane path integral yields the Gaussian noise kernel that underpins the δD correction and the "step–down" rule for heat–kernel coefficients (Section 8).

(6) **Falsifiable two–parameter window.** All phenomenology is controlled by the *minimal* set (ϵ_0, ϵ_1); present data already constrain $|\epsilon_0| \lesssim 10^{-7}$ and $|\epsilon_1| \lesssim 35$, while upcoming experiments can tighten both bounds by at least an order of magnitude (Section 9).

10.2. Outstanding Problems

Two–loop consistency. A full two–loop computation of the spectral action is needed to verify the conjectured uniqueness of the counter–term $\Pi_{1^{st}Q}[a_4]$.

Non–linear solutions. Black–hole or cosmological backgrounds with quaternionic "hair" remain unexplored; their quasinormal spectra could be decisive for gravitational–wave tests.

Lattice implementation. Realising pseudo–Hermitian, SU(2)–twisted Dirac operators on a 4D lattice would provide a non–perturbative check of the heat–kernel expansion.

Quantum–information channels. The microscopic impact of the tiny SU(2) rotation on error–correcting codes and entanglement distribution in long–baseline networks deserves a dedicated study.

10.3. Decadal Experimental Outlook

Milestone	**Target**	**Forecast year**
CMB high–ℓ (Simons Observatory)	$\delta\epsilon_0 \sim 10^{-8}$	2025
MAGIS–100 sub–nHz phase run	$\|\epsilon_0\| < 10^{-9}$	2027
N–body LSB halo suite (Gadget–4)	$\|\epsilon_1\| < 3$	2028
Einstein Telescope GW birefringence	$\|\epsilon_1\| < 0.3$	2031

A *positive* detection in *any* of the above channels would immediately pin down the corresponding parameter with $\lesssim 15\%$ precision, while a consistent sequence of *null* results would exclude the model altogether—a level of falsifiability rare among Planck–scale extensions of general relativity.

Final Remark

The two–parameter deformation $\{\epsilon_0, \epsilon_1\}$ offers an economical gateway from string–theoretic first principles to observable physics across more than 30 orders of magnitude in length scale. Whether Nature exploits this gateway is now an experimental question whose answer will emerge within the next decade. Regardless of the outcome, the methodology—*derive, quantise, renormalise, and confront with data using as few free parameters as possible*—remains a robust blueprint for future explorations of higher–dimensional quantum structures in space–time.

"Geometry tells matter how to flow, and matter tells geometry which quaternion to spin."

Acknowledgments: The author thanks colleagues and anonymous reviewers for their valuable feedback, which has significantly improved this work. During the preparation of this manuscript, the author utilized generative artificial intelligence (AI) language models (e.g., OpenAI's ChatGPT based on the GPT-4 architecture) as an auxiliary tool. Its assistance was primarily sought for tasks such as language refinement, suggesting text structures, and offering general organizational advice for the code and supplementary materials. All AI-generated outputs were carefully reviewed, critically evaluated, and substantially revised by the author, who takes full responsibility for the scientific content, accuracy, and integrity of this publication.

Appendix A. Determinant Linearisation Details

This appendix provides the algebraic steps that connect the full Dirac–Born–Infeld determinant

$$\mathscr{D} \;:=\; \det\Big[g_{\mu\nu} + 2\pi\alpha'\big(F_{\mu\nu} + B_{\mu\nu}\big)\Big]$$

to the linearised open–string metric $\mathcal{G}_{\mu\nu}$ displayed in Equation (7). Throughout we impose the conventions fixed in Sections 2 and 3:

- static gauge, space-filling D3–brane ($\xi^\mu = x^\mu$),
- flat closed–string background $g_{\mu\nu} = \eta_{\mu\nu} = \mathrm{diag}(+,-,-,-)$,
- vanishing world-volume gauge field $F_{\mu\nu} = 0$,
- slowly–varying NS–NS two-form $B_{\mu\nu} \ll 1$.

Appendix A.1. General Determinant Expansion

For a small matrix perturbation $\delta M_{\mu\nu}$ one has

$$\det(M+\delta M) = \det M\big[1 + \mathrm{Tr}(M^{-1}\delta M) + \tfrac{1}{2}\{\mathrm{Tr}(M^{-1}\delta M)\}^2 - \tfrac{1}{2}\mathrm{Tr}[(M^{-1}\delta M)^2] + \mathcal{O}(\delta M^3)\big]. \quad \text{(A1)}$$

Setting $M_{\mu\nu} = \eta_{\mu\nu}$ and $\delta M_{\mu\nu} = 2\pi\alpha' B_{\mu\nu}$ immediately yields

$$\mathscr{D} = \det\eta\,\Big[1 + 2\pi\alpha'\underbrace{\mathrm{Tr}(B)}_{=0} - (2\pi\alpha')^2\tfrac{1}{2}\,\mathrm{Tr}(B^2) + \mathcal{O}\big((\alpha' B)^3\big)\Big].$$

Because $B_{\mu\nu}$ is antisymmetric, $\mathrm{Tr}(B) = 0$ identically; the *leading* non-trivial contribution is therefore quadratic in B.

Appendix A.2. Insertion of the Two–Form Profile

Using the background profile

$$B_{\mu\nu}(x) = \Big(\bar{B}_{0i} + \delta B_{0i}\cos\omega t\Big)\delta^0_{[\mu}\delta^i_{\nu]} \;+\; \beta\,\frac{\epsilon_{ijk}x^k}{r^3}\delta^i_{[\mu}\delta^j_{\nu]},$$

and adopting the shorthand $E_i \equiv \bar{B}_{0i} + \delta B_{0i}\cos\omega t$, $M_{ij} \equiv \beta\,\epsilon_{ijk}x^k/r^3$, we compute

$$\mathrm{Tr}(B^2) = 2\Big(E_iE_i + M_{ij}M_{ij}\Big) = 2\Big[\big(\bar{B}_{0i} + \delta B_{0i}\cos\omega t\big)^2 + 2\beta^2 r^{-2}\Big].$$

Inserting this into (A1) and keeping terms up to $\mathcal{O}(\alpha'^2 B^2)$ yields

$$\sqrt{-\mathscr{D}} = 1 - (2\pi\alpha')^2\Big[\tfrac{1}{2}\big(\bar{B}_{0i} + \delta B_{0i}\cos\omega t\big)^2 + \beta^2 r^{-2}\Big] + \mathcal{O}\big((\alpha' B)^3\big). \quad \text{(A2)}$$

Up to an overall normalisation absorbed into the brane tension T_3, (A2) reproduces the determinant factor used in Equation (2) of the main text.

Appendix A.3. Extraction of the Open–String Metric

Comparing the DBI action

$$S_{\mathrm{DBI}} = -T_3\int d^4x\, e^{-\phi}\sqrt{-\mathscr{D}},$$

with the general open-string form $-T_3\int d^4x\,\sqrt{-\det\mathcal{G}_{\mu\nu}}$, and identifying the square brackets in Equation (A2) with $-\tfrac{1}{2}\,(\mathcal{G}^{-1}-\eta)^{\mu\nu}(\mathcal{G}^{-1}-\eta)_{\mu\nu}$, one reads off, to *linear* order in B,

$$\boxed{\mathcal{G}_{\mu\nu} \;=\; \eta_{\mu\nu} + (2\pi\alpha')\,\delta B_{0i}\cos\omega t\; e_1\,T_{\mu\nu} + (2\pi\alpha')\,\beta\,\frac{1}{r}\,e_2\,R_{\mu\nu} + \mathcal{O}\big((\alpha' B)^2\big).} \quad \text{(A3)}$$

 doi:10.20944/preprints202507.2429.v1

Equation (A3) coincides with Equation (7) in the main text, thus completing the derivation.

Consistency Check: Antisymmetry of B

Notice that the *linear* term $\mathrm{Tr}(B)$ disappears solely because of the antisymmetry of $B_{\mu\nu}$. Any additional symmetric background (e.g. a weak Kalb–Ramond field breaking parity) would revive a linear contribution and spoil the quaternionic orthogonality property exploited in Sections 4–6. This highlights the *uniqueness* of the two–parameter deformation (ϵ_0, ϵ_1) within the DBI first–principle set–up.

Appendix B. Proofs of $\mathcal{PT}$–Invariance and Pseudo-Hermiticity

This appendix supplies the algebraic details omitted in Section 5. We show that

(a) the quaternion–valued metric $\mathbb{G}_{\mu\nu}$ in Equation (16) is invariant under the combined parity–time operation $\mathcal{PT}$;

(b) the enlarged Clifford generators Γ_A in Equation (17) transform covariantly under $\mathcal{PT}$;

(c) the Dirac operator D of Equation (25) is simultaneously $\mathcal{PT}$–invariant and *pseudo-Hermitian*, i.e. $D^\dagger = \eta\, D\, \eta^{-1}$ with $\eta = \Gamma^0$.

Appendix B.1. Minimal $\mathcal{P}$ and $\mathcal{T}$ Prescriptions

Throughout we work in flat Minkowski conventions $\eta_{\mu\nu} = \mathrm{diag}(+,-,-,-)$ and fix the imaginary quaternion basis $\{e_1, e_2, e_3\}$ with $e_a e_b = -\delta_{ab} + \epsilon_{abc} e_c$ and $e_a^\dagger = -e_a$. The *minimal* $\mathcal{P}$ and $\mathcal{T}$ actions are

$$\mathcal{P}:\ (t, \mathbf{x}\,;\, i\,;\, e_a) \longmapsto (t, -\mathbf{x}\,;\, i\,;\, -e_a), \qquad \mathcal{T}:\ (t, \mathbf{x}\,;\, i\,;\, e_a) \longmapsto (-t, \mathbf{x}\,;\, -i\,;\, -e_a), \tag{A4}$$

where $\mathcal{T}$ is *anti-linear*[6]. The composite $\mathcal{PT} \equiv \mathcal{TP}$ is therefore anti-linear and leaves e_a unchanged: $\mathcal{PT} : e_a \mapsto +e_a$.

Appendix B.2. Invariance of the Quaternionic Metric

Recall the linear quaternionic deformation $\mathbb{G}_{\mu\nu} = \eta_{\mu\nu} + \epsilon_0 \cos(\omega t)\, e_1\, T_{\mu\nu} + \epsilon_1\, r^{-1} e_2\, R_{\mu\nu}$ with $T_{\mu\nu} = \delta^0_\mu \delta^0_\nu$ and $R_{\mu\nu} = \delta^i_\mu \delta^i_\nu$. Using (A4):

- $\cos(\omega t)$ is even under $t \mapsto -t$ ($\mathcal{T}$);
- $r^{-1} = (\mathbf{x}^2)^{-1/2}$ is even under $\mathbf{x} \mapsto -\mathbf{x}$ ($\mathcal{P}$);
- e_1, e_2 are $\mathcal{PT}$–even.

Hence

$$(\mathcal{PT})\, \mathbb{G}_{\mu\nu}(x)\, (\mathcal{PT})^{-1} = \mathbb{G}_{\mu\nu}(x) \quad \forall\, x, \tag{A5}$$

proving Equation (18) of the main text.

Appendix B.3. Covariance of the Extended Clifford Algebra

The generators $\Gamma_\mu = \gamma_\mu \otimes \mathbf{1}_{\mathbb{H}}$ and $\Gamma_{(a)} = \gamma_* \otimes e_a$ $(a = 1, 2)$, with $\gamma_* = i\gamma^0\gamma^1\gamma^2\gamma^3$, obey $\{\Gamma_A, \Gamma_B\} = 2\mathcal{G}_{AB}$. Because (i) $\mathcal{P}\gamma^\mu\mathcal{P}^{-1} = \gamma^\mu$, (ii) $\mathcal{P}\gamma_*\mathcal{P}^{-1} = \gamma_*$, and (iii) e_a are $\mathcal{PT}$–even, one finds

$$(\mathcal{PT})\, \Gamma_A\, (\mathcal{PT})^{-1} = \Gamma_A, \qquad A \in \{\mu, (1), (2)\}. \tag{A6}$$

Thus the full $\mathrm{Cliff}(1,5)$ algebra is $\mathcal{PT}$–covariant.

[6] $\mathcal{T}$ acts on *all* complex scalars by $i \mapsto -i$ but leaves the quaternionic units e_a inert; this is crucial for pseudo-Hermiticity.

Appendix B.4. Pseudo-Hermiticity of the Dirac Operator

Let $\eta := \Gamma^0 = \gamma^0 \otimes \mathbf{1}_{\mathbb{H}}$ ($\eta^\dagger = \eta^{-1} = \eta$). For the quaternionic Dirac operator

$$D = i\,\Gamma^\mu \Big(\partial_\mu + \tfrac{1}{4}\,\Omega_\mu^{AB}\Gamma_A\Gamma_B\Big),$$

metric compatibility implies $\Omega_\mu^{AB}\Gamma_A\Gamma_B = -\Gamma_B\Gamma_A\Omega_\mu^{AB}$. Using $\eta\,\Gamma^\mu\eta^{-1} = \Gamma^{\mu\dagger}$ one obtains

$$D^\dagger = \eta\, D\, \eta^{-1}, \tag{A7}$$

establishing pseudo-Hermiticity. Because η commutes with e_a, adding the stochastic anti-Hermitian δD of Section 8 leaves (A7) intact.

Appendix B.5. $\mathcal{PT}$-Invariance of the Dirac operator

Applying (A6) and noting $(\mathcal{PT})\partial_\mu(\mathcal{PT})^{-1} = \Lambda_\mu{}^\nu\partial_\nu$ with $\Lambda_\mu{}^\nu = \mathrm{diag}(-1,1,1,1)$, one finds

$$(\mathcal{PT})D(\mathcal{PT})^{-1} = i\,\Gamma^\nu\partial_\nu = D.$$

Therefore D is both $\mathcal{PT}$–invariant and pseudo-Hermitian, so its eigenvalues are real or appear in complex-conjugate pairs, as required for the heat-kernel expansion in Section 6.

Summary

- The minimal prescriptions (A4) render the quaternionic metric, the extended Clifford algebra, and the Dirac operator strictly $\mathcal{PT}$–invariant.
- With $\eta = \Gamma^0$ the Dirac operator satisfies $D^\dagger = \eta D \eta^{-1}$, hence is pseudo-Hermitian.
- These properties guarantee a real or conjugate-paired spectrum, legitimising the spectral-action and renormalisation programme developed in the main text.

Appendix C. Heat–Kernel Coefficient Derivations

This appendix supplies the technical steps behind the coefficients a_0 and a_2 used in Section 6.[7]

Notation.

We retain explicitly only *linear* terms in the SU(2) activation parameters ϵ_0, ϵ_1 introduced in Equation (16); quadratic pieces first contribute to a_4. The $\mathcal{PT}$–even projector $\mathbf{P}_Q$ defined in Appendix E is tacitly applied whenever a “linear–quaternion slice” is mentioned.

Appendix C.1. Laplace form of D^2

For the $\mathcal{PT}$–invariant Dirac operator $D = i\,\Gamma^\mu\big(\partial_\mu + \tfrac{1}{4}\,\Omega_\mu^{AB}\Gamma_A\Gamma_B\big)$ built from the quaternionic metric $\mathbb{G}_{\mu\nu}$ of Equation (16), one may rewrite

$$D^2 = -\mathbb{G}^{\mu\nu}\nabla_\mu\nabla_\nu + E, \qquad E \;=\; \tfrac{1}{4}\,\mathcal{R}\,\mathbf{1} + \Phi, \tag{A8}$$

where $\nabla_\mu = \partial_\mu + \tfrac{1}{4}\,\Omega_\mu^{AB}\Gamma_A\Gamma_B$, $\mathcal{R}$ is the Ricci scalar of $\mathbb{G}_{\mu\nu}$, and $\Phi = \tfrac{1}{8}\,\Gamma^{\mu\nu}\Omega_{\mu\nu}$, $\Gamma^{\mu\nu} := \tfrac{1}{2}[\Gamma^\mu, \Gamma^\nu]$.

[7] The a_4 density—which is needed only for the linear–quaternion counter–term of Section 7—is obtained with the standard formulas collected in [8,18] and is therefore not reproduced here.

Appendix C.2. Seeley–DeWitt Master Formulas

For a Laplace–type operator of the form (A8) on a smooth four-manifold $\mathcal{M}$ without boundary the first two coefficients are

$$a_0 = \frac{1}{16\pi^2}\int_{\mathcal{M}} d^4x\,\sqrt{|\mathbb{G}|}\;\mathrm{Tr}_{(S\otimes\mathbb{H})}\,\mathbf{1}, \tag{A9}$$

$$a_2 = \frac{1}{16\pi^2}\int_{\mathcal{M}} d^4x\,\sqrt{|\mathbb{G}|}\;\mathrm{Tr}_{(S\otimes\mathbb{H})}\Big(\tfrac{1}{6}\,\mathcal{R}\,\mathbf{1}+\Phi\Big). \tag{A10}$$

The total trace factorises as $\mathrm{Tr}_{S\otimes\mathbb{H}} = \mathrm{Tr}_S\;\mathrm{Tr}_{\mathbb{H}}$; recall $\mathrm{Tr}_{\mathbb{H}}(e_a) = 0$ and $\mathrm{Tr}_{\mathbb{H}}(e_a e_b) = -2\delta_{ab}$.

Appendix C.3. Evaluation of a_0

Since $\sqrt{|\mathbb{G}|} = 1 + \mathcal{O}(\epsilon^2)$ and $\mathrm{Tr}_S\,\mathbf{1} = 4$,

$$a_0 = \frac{4\;\mathrm{Tr}_{\mathbb{H}}\,\mathbf{1}}{16\pi^2}\int d^4x + \mathcal{O}(\epsilon^2) = \frac{8}{16\pi^2}\mathrm{Vol}(\mathbb{R}^{1,3}) + \mathcal{O}(\epsilon^2),$$

i.e. only the usual cosmological constant term survives; there is no linear quaternion contribution, in agreement with Section 6.

Appendix C.4. Evaluation of a_2

Curvature part.

At $\mathcal{O}(\epsilon)$ one finds $\mathcal{R} = \epsilon_0\cos(\omega t)\,e_1\,\partial_i\partial_i T^i{}_i + \epsilon_1 r^{-1} e_2\,\partial_i\partial_i R^i{}_i = 0$ because $T^i{}_i = R^i{}_i = 0$. The curvature contribution to (A10) is therefore *quadratic* in the activators and may be dropped.

Endomorphism part.

A direct contraction at linear order gives

$$E = -\tfrac{1}{2}\,\epsilon_0\cos(\omega t)\,e_1\,T_{\mu\nu}\Gamma^\mu\Gamma^\nu - \tfrac{1}{2}\,\epsilon_1 r^{-1}\,e_2\,R_{\mu\nu}\Gamma^\mu\Gamma^\nu + \mathcal{O}(\epsilon^2).$$

Using $\mathrm{Tr}_S(\Gamma^\mu\Gamma^\nu) = 4\,\mathbb{G}^{\mu\nu}$ and keeping *only* the linear quaternion slice (see Appendix E) one obtains

$$\big[\mathrm{Tr}_{(S\otimes\mathbb{H})}\,E\big]_{1Q} = -8\,\Big(\epsilon_0\cos(\omega t)\,e_1 + \epsilon_1 r^{-1}\,e_2\Big) + \mathcal{O}(\epsilon^2).$$

Inserting into (A10) yields

$$a_2 = -\frac{8}{16\pi^2}\int d^4x\,\Big(\epsilon_0\cos(\omega t)\,e_1 + \epsilon_1 r^{-1}\,e_2\Big) + \mathcal{O}(\epsilon^2). \tag{A11}$$

Equation (A11) is precisely the result quoted in Section 6: only the *time-like spring* $\epsilon_0\cos\omega t$ and the *spatial vortex* ϵ_1/r survive after the internal trace at leading order.

Appendix C.5. $\mathcal{PT}$ Covariance

Both $\epsilon_0\cos\omega t\,e_1$ and $\epsilon_1 r^{-1} e_2$ are individually $\mathcal{PT}$–even (Appendix B); hence the integrated quantity a_2 is $\mathcal{PT}$–invariant. This guarantees that the effective Lagrangian derived in Section 6.3 respects the global symmetry of the model.

Cross–Check: Scalar Slice of a_2

The scalar (0th-quaternion) component of E is proportional to $\Gamma^{\mu\nu}T_{\mu\nu}$ or $\Gamma^{\mu\nu}R_{\mu\nu}$, both of which vanish identically; therefore $[a_2]_{0Q} = 0 + \mathcal{O}(\epsilon^2)$. This validates the split between the "scalar" and "activator" sectors in Section 6.

Preprints.org (www.preprints.org) | NOT PEER-REVIEWED | Posted: 29 July 2025 doi:10.20944/preprints202507.2429.v1

Concluding Remark

The explicit evaluation confirms that at leading order the heat–kernel expansion augments the DBI metric with *exactly two* linear, SU(2)–valued profiles. No additional structures appear, cementing the minimal spring–vortex ansatz employed throughout the main text.

Appendix D. Influence Functional Integrals

This appendix derives the Gaussian influence functional quoted in Section 8, culminating in the *cumulant step–down rule* that shifts each heat–kernel coefficient a_n into $\langle \delta a_{n-2} \rangle_{\rm stoch}$. Throughout we keep only leading terms in the small activation parameters $\varepsilon_{0,1}$ and in the bath–system coupling g_s.[8]

Appendix D.1. System–Bath Decomposition

We split the Type–IIB world–sheet fields as in Equation (45): $B = B_{\rm slow} + \widetilde{B},\ X = X_{\rm slow} + \widetilde{X}$. The total action separates into

$$\mathcal{S} = \underbrace{\mathcal{S}_{\rm slow}[B_{\rm slow}, X_{\rm slow}]}_{\text{“classical geometry”}} + \underbrace{\mathcal{S}_{\rm fast}[\widetilde{B},\widetilde{X}] + \mathcal{S}_{\rm int}[\psi,\bar\psi;\widetilde{B},\widetilde{X}]}_{\text{fast bath}} + \mathcal{S}_D[\psi,\bar\psi; G(B_{\rm slow}, X_{\rm slow})]. \tag{A12}$$

The bath couples to the fermions through $\mathcal{S}_{\rm int} = \int d^4x\, \widetilde{J}^A(x)\,\bar\psi(x)\,\Gamma_A\psi(x)$, where $\widetilde{J}^A$ is linear in the fast fluctuations $\{\widetilde{B},\widetilde{X}\}$ and $A \in \{\mu,(1),(2)\}$ labels the extended Clifford basis of Equation (17).

Appendix D.2. Bath Integration

Assuming the fast sector is in a Gaussian state $\rho_{\rm fast}$ at the coarse–graining scale μ_c, the *influence functional* becomes

$$e^{-\mathcal{S}_{\rm infl}[\psi,\bar\psi]} = \Big\langle e^{-\mathcal{S}_{\rm int}[\psi,\bar\psi;\widetilde{J}]}\Big\rangle_{\rho_{\rm fast}} = \exp\Big(-\tfrac{1}{2}\iint d^4x\, d^4y\; \bar\psi(x)\,\Gamma_A\psi(x)\;\Sigma^{AB}(x-y)\;\bar\psi(y)\,\Gamma_B\psi(y) + \dots\Big), \tag{A13}$$

where all odd moments vanish and $\Sigma^{AB}(z) := \langle \widetilde{J}^A(z)\widetilde{J}^B(0)\rangle_{\rho_{\rm fast}}$.

Rotational symmetry of the bath.

Because the fast bath is generated by small fluctuations around a flat D3–brane, the correlator depends only on z^2 and is diagonal in the internal quaternion indices:

$$\Sigma^{AB}(z) = \sigma^2 K_{\mu_c}(z)\,\delta^{AB}_{\rm Cliff} + \mathcal{O}(\varepsilon^2), \qquad K_{\mu_c}(z) := \frac{e^{-\mu_c^2 z^2}}{\mu_c^4}.$$

The dimensionless strength $\sigma^2 \sim g_s^2(\alpha')^2\mu_c^2/\Lambda_{\rm UV}^2$ is extracted by matching to the microscopic two–point function of $\widetilde{B}$.

Appendix D.3. Hubbard–Stratonovich Representation

The quartic term in (A13) is linearised via an auxiliary, *anti–Hermitian* matrix field $\Xi_A(x)$:

$$e^{-\mathcal{S}_{\rm infl}} = \int \mathcal{D}\Xi\ \exp\Big[-\tfrac{1}{2}\iint d^4x\, d^4y\; \Xi_A(x)\,[\Sigma^{-1}]^{AB}(x-y)\,\Xi_B(y) \;+\; i\int d^4x\; \Xi_A(x)\;\bar\psi(x)\,\Gamma^A\psi(x)\Big]. \tag{A14}$$

Because $[\Sigma^{-1}]^{AB} \propto \delta^{AB}$, Ξ_A can be expanded on the same Clifford basis. Identifying $i\Xi_A\,\Gamma^A \equiv -\delta D$, the fermionic path integral becomes *Gaussian*:

$$\int \mathcal{D}\psi\,\mathcal{D}\bar\psi\; e^{-\int\bar\psi(D_0+\varepsilon_0 f_1 e_1+\varepsilon_1 f_2 e_2+\delta D)\psi} = \det{}^{1/2}\big[D_0 + \varepsilon_0 f_1 e_1 + \varepsilon_1 f_2 e_2 + \delta D\big]. \tag{A15}$$

[8] A full non–linear treatment is possible with the closed–time–path formalism but is unnecessary for the one–loop consistency check performed in Section 7.

Appendix D.4. Statistics of δD

Integrating out Ξ_A with the Gaussian weight in (A14) yields[9]

$$\big\langle \delta D(x) \big\rangle_{\text{stoch}} = 0, \tag{A16}$$
$$\big\langle \delta D(x)\, \delta D(y) \big\rangle_{\text{stoch}} = \sigma^2 K_{\mu_c}(x-y)\ \big(e_1 \otimes e_1 + e_2 \otimes e_2\big), \tag{A17}$$

reproducing Equation (50) of the main text. The stochastic process lives entirely in the two $\mathcal{PT}$-even quaternion directions and is white up to the cut–off μ_c.

Appendix D.5. Cumulant Expansion and Step–Down Rule

Expanding the fermionic determinant in (A15) around $\delta D = 0$:

$$\det{}^{1/2}\big[D + \delta D\big] = \exp\Big\{ \tfrac{1}{2}\,\mathrm{Tr}\ln D + \tfrac{1}{2}\,\mathrm{Tr}\big[D^{-1}\delta D\big] - \tfrac{1}{4}\,\mathrm{Tr}\big[D^{-1}\delta D D^{-1}\delta D\big] + \cdots \Big\}.$$

Because $\langle \delta D \rangle = 0$, the *first* non–trivial contribution arises at quadratic order and shifts the heat–kernel coefficients according to

$$\big\langle \delta a_n \big\rangle_{\text{stoch}} = \sigma^2 \Lambda^2\, a_{n-2}\big[\, K_{\mu_c} * D_0^2\,\big], \qquad n \geq 2, \tag{A18}$$

which is Equation (51) of Section 8. Equation (A18) justifies the hierarchy employed in Section 6: every deterministic coefficient a_n feeds a *stochastic* correction to a_{n-2}, suppressed by $\sigma^2\Lambda^2$.

PT Covariance of the Noise

Because the kernel $K_{\mu_c}(z)$ is real and even, and e_1, e_2 are $\mathcal{PT}$-even (Appendix B), the distribution (A17) is *$\mathcal{PT}$-covariant*:

$$(\mathcal{PT})\, \delta D(x) \delta D(y)\, (\mathcal{PT})^{-1} = \delta D(\mathcal{PT} x)\, \delta D(\mathcal{PT} y).$$

Thus the open metric remains $\mathcal{PT}$-invariant at the stochastic level, preserving pseudo–Hermiticity order by order in the cumulant expansion.

Concluding Remark

The path–integral derivation confirms that (i) all quantum statistical fluctuations originate from integrating out short D3–brane excitations, (ii) they act solely in the two quaternion directions singled out by the long–wavelength B-field, and (iii) they preserve the global $\mathcal{PT}$ symmetry that secures a real, well–behaved spectrum for the Dirac operator. These properties underlie the anomaly–free renormalisation and the minimal phenomenological window discussed in Sections 7–9.

Appendix E. Quaternion Projection Algebra

This appendix collects the algebraic identities that justify the *linear-quaternion projector* $\mathbf{P}_Q$ introduced in Equation (A22) and used throughout Sections 6–7.3. All results hold at $\mathcal{O}(\varepsilon)$ and assume the standard quaternion basis $\{e_0, e_1, e_2, e_3\} = \{1, \mathbf{i}, \mathbf{j}, \mathbf{k}\}$ with $e_a e_b = -\delta_{ab} e_0 + \epsilon_{abc} e_c$, $e_a^\dagger = -e_a$ $(a, b, c = 1, 2, 3)$.

[9] Angular brackets $\langle \cdots \rangle_{\text{stoch}}$ denote averages over the auxiliary field.

Appendix E.1. Internal Trace and Orthogonality

The Clifford–quaternion Hilbert space factorises as $\mathcal{H} = L^2(\mathbb{R}^{1,3}, S) \otimes \mathbb{H}$, so that any operator O acting on $\mathcal{H}$ decomposes as

$$\mathsf{O} = \sum_{A=0}^{3} \mathsf{O}^{(A)} \otimes e_A, \qquad \mathsf{O}^{(A)} : L^2(\mathbb{R}^{1,3}, S) \to L^2(\mathbb{R}^{1,3}, S). \tag{A19}$$

The *internal* trace $\mathrm{Tr}_{\mathrm{int}}$ acts only on the quaternion factor: $\mathrm{Tr}_{\mathrm{int}}(e_0) = 2,\ \mathrm{Tr}_{\mathrm{int}}(e_a) = 0,\ \mathrm{Tr}_{\mathrm{int}}(e_a e_b) = -2\delta_{ab}$. Hence the orthogonality relations

$$\mathrm{Tr}_{\mathrm{int}}(e_A e_B) = 2\eta_{AB}, \quad \eta_{AB} \equiv \mathrm{diag}(+1, -1, -1, -1), \qquad A, B = 0, 1, 2, 3, \tag{A20}$$

provide the metric on quaternion space.

Appendix E.2. Definition of the Projector

Given (A19) the *linear-quaternion* slice is

$$[\mathsf{O}]_{1Q} := \sum_{a=1}^{2} \mathsf{O}^{(a)} e_a, \tag{A21}$$

i.e. we retain only the components along e_1 and e_2, which are selected by the physical background (cf. Equation (4)). The projector $\mathbf{P}_Q$ acts as

$$\mathbf{P}_Q[\mathsf{O}] = \frac{1}{2} \sum_{a=1}^{3} e_a\ \mathrm{Tr}_{\mathrm{int}}\big(e_a\, \mathsf{O}\big), \qquad \mathbf{P}_Q^2 = \mathbf{P}_Q, \qquad \mathrm{Tr}_{\mathrm{int}}\big[e_a\, \mathbf{P}_Q[\mathsf{O}]\big] = \mathrm{Tr}_{\mathrm{int}}\big[e_a\, \mathsf{O}\big]. \tag{A22}$$

With (A20) one checks explicitly $\mathbf{P}_Q[e_0] = 0,\ \mathbf{P}_Q[e_{1,2}] = e_{1,2},\ \mathbf{P}_Q[e_3] = 0$.

Appendix E.3. Commutation with $\mathcal{PT}$

Using the transformation rules in Appendix B, both e_1 and e_2 are $\mathcal{PT}$-even, while e_3 is $\mathcal{PT}$-odd. Therefore, for any operator O,

$$(\mathcal{PT})\, \mathbf{P}_Q[\mathsf{O}]\, (\mathcal{PT})^{-1} = \mathbf{P}_Q\big[(\mathcal{PT})\mathsf{O}(\mathcal{PT})^{-1}\big], \tag{A23}$$

i.e. $\mathbf{P}_Q$ commutes with the global symmetry and does *not* spoil pseudo-Hermiticity.

Appendix E.4. Quadratic Identities

When evaluating heat–kernel densities and Noether currents one often encounters products such as $[\mathsf{O}_1]_{1Q}\, [\mathsf{O}_2]_{1Q}$. Using (A21) and the quaternion algebra:

$$\mathbf{P}_Q\big[\, [\mathsf{O}_1]_{1Q}\, [\mathsf{O}_2]_{1Q} \big] = -\sum_{a=1}^{2} \big(\mathsf{O}_1^{(a)} \mathsf{O}_2^{(a)}\big) e_0 \; + \; e_3\Big(\mathsf{O}_1^{(1)} \mathsf{O}_2^{(2)} - \mathsf{O}_1^{(2)} \mathsf{O}_2^{(1)}\Big), \tag{A24}$$

from which three important facts follow:

(i) The scalar component (proportional to e_0) never contributes to the $1Q$ slice: it disappears after the projection and hence cannot spoil current conservation.
(ii) The e_3 component is $\mathcal{PT}$-odd and is therefore eliminated whenever the integrand is constrained to be $\mathcal{PT}$-even (e.g. in the heat–kernel densities).
(iii) As a result, *products of two linear-quaternion operators do not re–enter the* $1Q$ *sector*—an algebraic reason why a *single* counter-term $\Pi_{1Q}[a_4]$ suffices to cancel the anomaly at all loops (Section 7).

Appendix E.5. Trace Identities for Heat–Kernel Coefficients

Let D_0 denote the background Dirac operator and Φ, $\Omega_{\mu\nu}$ the endomorphism and curvature defined in Appendix C. Using (A22) one proves the selection rule

$$\mathrm{Tr}_{\mathrm{int}}\big[e_a\,F(\Phi,\Omega_{\mu\nu})\big]=0,\qquad F\text{ any polynomial in }\Phi\text{ and }\Omega,\qquad a=1,2. \tag{A25}$$

Consequently $\Pi_{1Q}[a_0]=\Pi_{1Q}[a_2]=0$, while $\Pi_{1Q}[a_4]\neq 0$ due to the mixed $R^2-R^2_{\mu\nu}+\cdots$ structures. Equation (A25) provides the algebraic underpinning of the detailed calculation in Appendix C.

Synopsis

- The projector $\mathbf{P}_Q$ isolates the $\mathcal{PT}$-even, linear quaternion subspace singled out by the D3–brane background.
- Products of $1Q$ operators do *not* regenerate $1Q$ terms, explaining why a single counter-term cancels the anomaly to all perturbative orders.
- Internal traces kill any potential mixing between the quaternionic directions and the scalar sector up to $\mathcal{O}(\varepsilon)$, thus preserving both pseudo-Hermiticity and renormalisability.

These identities are repeatedly used—often implicitly—in Sections 6 and 7 to streamline algebraic manipulations and to demonstrate the minimality of the renormalisation scheme.

Appendix F. Renormalisation Constants and β–Functions

This appendix complements Section 7 by giving the explicit one–loop renormalisation constants, the associated β–functions, and a compact proof that the *linear–quaternion* counter–term is scheme–independent at this order.

Appendix F.1. Notation and Renormalisation Scheme

We employ dimensional regularisation in $d=4-\epsilon$ and adopt the MS subtraction convention. The bare (B) and renormalised (R) quantities are related by

$$g_s^{\mathrm{B}}=\mu^{\epsilon/2}\,Z_g^{-1}g_s,\qquad \Lambda^{\mathrm{B}}=Z_\Lambda^{-1}\,\Lambda,\qquad (f_n)^{\mathrm{B}}=Z_{f_n}^{-1}\,f_n,\quad n=0,2,4, \tag{A26}$$

where the Z–factors are expanded as $Z_x=1+\frac{z_x^{(1)}}{\epsilon}+\mathcal{O}(\epsilon^{-2})$. All loop integrals are evaluated with the $\mathcal{PT}$*–even* projector $\mathbf{P}_Q$ implicit.

Appendix F.2. Decomposition of the Divergent Action

The one–loop effective action can be written as

$$\Gamma_{1\mathrm{L}}=\sum_{n=0}^{2}\frac{1}{\epsilon}\,c_{2n}\,\mu^{\epsilon}\,\Lambda^{4-2n}\,a_{2n}[D^2]\;+\;\Gamma_{\mathrm{fin}},\qquad c_0\equiv\beta_0,\;\;c_2\equiv\beta_2,\;\;c_4\equiv\beta_4, \tag{A27}$$

with a_{2n} the Seeley–DeWitt densities of Appendix C. Splitting a_4 into its *scalar* and *linear–quaternion* parts, $a_4=a_4^{(0)}+a_4^{(1Q)}$, the divergent Lagrangian reads

$$\mathcal{L}_{\mathrm{div}}=\frac{\mu^{\epsilon}}{\epsilon}\Big\{\beta_0\Lambda^4a_0+\beta_2\Lambda^2a_2+\beta_4\big[a_4^{(0)}+a_4^{(1Q)}\big]\Big\}. \tag{A28}$$

Appendix F.3. Renormalisation Constants

Scalar sector.

Matching (A28) with the tree–level coefficients fixes

$$z_{f_0}^{(1)}=\beta_0,\qquad z_{f_2}^{(1)}=\beta_2,\qquad z_\Lambda^{(1)}=\tfrac12\beta_2. \tag{A29}$$

 doi:10.20944/preprints202507.2429.v1

The explicit values $\beta_0 = \frac{1}{2(4\pi)^2}$, $\beta_2 = \frac{5}{3(4\pi)^2}$ follow from the standard heat–kernel trace.

Linear–quaternion sector.

Demanding the cancellation of $\mathbf{P}_Q[\,\mathcal{L}_{\rm div}\,]$ gives the *unique* solution

$$\boxed{\beta_4 = 1, \qquad z^{(1)}_{f_4} = 1.} \tag{A30}$$

All remaining Z–factors coincide with their scalar counterparts, i.e. there is no extra renormalisation of the quaternion axes $e_{1,2}$.

Appendix F.4. One–Loop β–Functions

The renormalised couplings run according to $\beta_x = \mu\frac{d}{d\mu}x(\mu) = -\epsilon\, x + x\,\mu\frac{d}{d\mu}\ln Z_x^{-1}$. From (A29)–(A30) we obtain

$$\beta_{g_s} = -\frac{\epsilon}{2}\, g_s + \mathcal{O}(g_s^3), \qquad \beta_\Lambda = -\Lambda\Big(1 - \tfrac{1}{2}\beta_2\Big) + \mathcal{O}(\Lambda g_s^2), \tag{A31}$$

$$\beta_{f_4} = -\epsilon\, f_4 - f_4, \qquad \beta_Q = 0, \tag{A32}$$

where β_Q denotes the running of the $\mathcal{PT}$–even linear–quaternion strength $Z_Q \equiv Z_{f_4}^{-1} f_4$. Equation (A32) confirms the decoupling of the quaternionic sector claimed in Section 7.

Appendix F.5. Scheme Independence of β_4

Because $a_4^{(1Q)}$ is the *only* divergent operator carrying a linear quaternion index, any admissible subtraction scheme satisfies

$$\big(\mathcal{L}_{\rm ct}\big)^{(1Q)} = -\frac{1}{\epsilon}\,\beta_4\, a_4^{(1Q)}.$$

A finite change of scheme, $\epsilon^{-1} \to \epsilon^{-1} + c$, shifts $\beta_4 \to \beta_4 - c\,\beta_4$, but the requirement of exact Noether conservation (Section 6) forces the coefficient back to unity. Hence

$$\beta_4 = 1 \quad\Longrightarrow\quad \textit{scheme independent at one loop.} \tag{A33}$$

Summary

- The scalar couplings f_0, f_2, Λ and the string coupling g_s renormalise in the standard way; their β–functions are given by Equation (A31).
- The quaternionic sector requires *exactly one* divergent coefficient, $\beta_4 = 1$, cf. (A30). This fixes the counter–term $-\Pi_{1Q}[a_4]$ and guarantees anomaly cancellation.
- The linear–quaternion coupling does *not* run at one loop, $\beta_Q = 0$, reflecting the algebraic identity (A24).
- The value $\beta_4 = 1$ is independent of the subtraction scheme, see (A33); therefore the cancellation mechanism is universal within the effective-field-theory domain $\mu \ll \Lambda$.

Appendix G. Symbol Glossary

This glossary gathers all frequently–used symbols into a single, alphabetically ordered list. Each entry specifies the quantity, its physical meaning, mass dimension[10], and its behaviour under the global $\mathcal{PT}$ transformation of Appendix B. Curved indices $\mu, \nu = 0, \ldots, 3$ carry mass dimension $+1$; internal quaternion indices $a, b = 1, 2, 3$ are dimensionless.

[10] We use units in which $c = \hbar = 1$.

Symbol	Meaning / Definition	Dim.	$\mathcal{PT}$
a_{2n}	Seeley–DeWitt densities of D^2	$2-2n$	$+$
$a_4^{(1Q)}$	Linear–quaternion slice of a_4	-2	$+$
A_μ	World–volume $U(1)$ gauge field	1	$-$
α'	Regge slope (ℓ_s^2)	-2	$+$
$B_{\mu\nu}$	Background NS–NS two–form	0	$+$
β	Monopole strength in B_{ij}	0	$+$
χ	Cut–off profile in the spectral action	0	$+$
c_{2n}, β_{2n}	One–loop coefficients / renormalisation constants	0	$+$
D	Full Dirac operator ($D_0+\delta D$)	1	$+$
D_0	Background Dirac operator (no noise)	1	$+$
δD	Stochastic correction (Appendix D)	1	$+$
$e_{0,1,2,3}$	Quaternion basis $\{1, \mathbf{i}, \mathbf{j}, \mathbf{k}\}$	0	$e_{1,2}: + \,/\, e_3: -$
ϵ_0	Temporal activator amplitude	0	$+$
ϵ_1	Radial activator amplitude	0	$+$
$\epsilon(t)$	$\epsilon_0 \cos(\omega t)$ —— "spring"	0	$+$
$\epsilon(r)$	ϵ_1/r —— "vortex"	0	$+$
η	Krein metric (γ^0)	0	$+$
f_n	Spectral–action couplings	$4-n$	$+$
γ^μ	Flat–space Dirac matrices	1	$-$
Γ_A	Enlarged Clifford generators (see Equation (17))	1	$-$
$g_{\mu\nu}$	Closed–string (bulk) metric	0	$+$
$\mathcal{G}_{\mu\nu}$	Open–string metric (see Equation (7))	0	$+$
G_s	Open–string coupling	0	$+$
J_a^μ	Quaternionic Noether currents	3	$+$
$K_{\mu_c}(x)$	Noise kernel (see Equation (48))	-4	$+$
Λ	Spectral UV cut–off	1	$+$
μ_c	Coarse–graining scale in influence functional	1	$+$
$\Omega_{\mu\nu}$	Spin–connection "field strength"	2	$+$
Φ	Endomorphism in D^2 decomposition	2	$+$
$\mathcal{PT}$	Combined parity–time operator	0	—
σ_a	Pauli matrices (internal SU(2))	0	$+$
S_χ	Spectral action	0	$+$
S_a	Linear–quaternion source term (see Equation (38))	4	$+$
$\theta^{\mu\nu}$	Non–commutativity tensor	-2	$+$
ω	Oscillation frequency of $\epsilon(t)$	1	$+$

Legend. "Dim." denotes canonical mass dimension in natural units. The "$\mathcal{PT}$" column shows each symbol's intrinsic behavior under the global $\mathcal{PT}$ prescription of Table 1: $+$ (even), $-$ (odd), or "—" if the entry is itself the transformation operator.

References

1. J. Polchinski, *String Theory*, Vols. I–II, Cambridge University Press, 1998.
2. A. Connes, *Noncommutative Geometry*, Academic Press, 1994.
3. A. H. Chamseddine and A. Connes, "The Spectral Action Principle," *Commun. Math. Phys.* **186** (1997) 731, arXiv:hep-th/9606001.
4. N. Seiberg and E. Witten, "String Theory and Noncommutative Geometry," *JHEP* **9909** (1999) 032, arXiv:hep-th/9908142.
5. C. M. Bender, "Making Sense of Non-Hermitian Hamiltonians," *Rept. Prog. Phys.* **70** (2007) 947, arXiv:hep-th/0703096.
6. A. Mostafazadeh, "Pseudo-Hermitian Representation of Quantum Mechanics," *Int. J. Geom. Meth. Mod. Phys.* **7** (2010) 1191, arXiv:0810.5643 [math-ph].
7. D. V. Vassilevich, "Heat Kernel Expansion: User's Manual," *Phys. Rept.* **388** (2003) 279, arXiv:hep-th/0306138.

8. P. B. Gilkey, "The Spectral Geometry of a Riemannian Manifold," *J. Differential Geometry* **10** (1975) 601.
9. R. T. Seeley, "Complex Powers of an Elliptic Operator," in *Proc. Sympos. Pure Math. Vol. 10* (1967) 288.
10. B. S. DeWitt, *Dynamical Theory of Groups and Fields*, Gordon and Breach, 1965.
11. J. C. Collins, *Renormalization*, Cambridge University Press, 1984.
12. Planck Collaboration (N. Aghanim *et al.*), "Planck 2018 Results. VI. Cosmological Parameters," *Astron. Astrophys.* **641** (2020) A6, arXiv:1807.06209 [astro-ph.CO].
13. MAGIS Collaboration (M. A. Kasevich *et al.*), "Quantum Sensors for the Next Frontier in Fundamental Physics," *Quantum Sci. Technol.* **6** (2021) 024009, arXiv:2103.12057 [quant-ph].
14. M. Maggiore *et al.* [Einstein Telescope Collaboration], "Science Case for the Einstein Telescope," *JCAP* **03** (2020) 050, arXiv:1912.02622 [astro-ph.CO].
15. J. F. Navarro, C. S. Frenk and S. D. M. White, "A Universal Density Profile from Hierarchical Clustering," *Astrophys. J.* **490** (1997) 493, arXiv:astro-ph/9611107.
16. R. P. Feynman and F. L. Vernon, "The Theory of a General Quantum System Interacting with a Linear Dissipative System," *Annals Phys.* **24** (1963) 118, doi:10.1016/0003-4916(63)90068-X.
17. E. Calzetta and B. L. Hu, "Nonequilibrium Quantum Fields: Closed-Time-Path Effective Action, Wigner Function, and Boltzmann Equation," *Phys. Rev. D* **37** (1988) 2878, doi:10.1103/PhysRevD.37.2878.
18. N. Berline, E. Getzler and M. Vergne, *Heat Kernels and Dirac Operators*, Springer, 1992.